Electrophoretic deposition of polymethylmethacrylate and composites for biomedical applications

A. D'Elia[a], J. Deering[a], A. Clifford[a], B.E.J. Lee[b], K. Grandfield[a,b], I. Zhitomirsky[a,b,*]

[a] *Department of Materials Science and Engineering, McMaster University, Hamilton, ON, L8S 4L7, Canada*
[b] *School of Biomedical Engineering, McMaster University, Hamilton, ON, L8S 4L7, Canada*

ARTICLE INFO

Keywords:
Electrophoretic deposition Polymethylmethacrylate Alumina
Sodium cholate Film
Implant
Cell proliferation Bioactivity

ABSTRACT

For the first time, an electrophoretic deposition (EPD) method has been developed for the deposition of polymethylmethacrylate (PMMA) and PMMA-alumina films for biomedical implant applications. The proposed biomimetic approach was based on the use of a bile salt, sodium cholate (NaCh), which served as a multifunctional solubilizing, charging, dispersing and film-forming agent. Investigations revealed PMMA-Ch^- and PMMA-alumina interactions, which facilitated the deposition of PMMA and PMMA-alumina films. This approach allows for the use of a non-toxic water-ethanol solvent for PMMA. The proposed deposition strategy can also be used for co-deposition of PMMA with other functional materials. The PMMA and composite films were tested for biomedical implant applications. The PMMA-alumina films showed statistically improved metabolic results compared to both the bare stainless steel substrate and pure PMMA films. Alkaline phosphatase (ALP) activity affirmed the bioactivity and osteoconductive potential of PMMA and composite films. PMMA-alumina films showed greater ALP activity than both the PMMA-coated and uncoated stainless steel.

1. Introduction

Polymethylmethacrylate (PMMA) is widely recognized as an advanced material for biomedical applications. This polymer exhibits important properties, such as biocompatibility, chemical stability, and a high Young's modulus [1]. Major applications included ophthalmology and orthopaedic devices, scaffolds, fillers for bone cavities, drug delivery systems, biosensors, bone and dental cements [2–5]. Addition of bioceramics, such as alumina, to PMMA was also found to be advantageous due to its ability to promote osteoblast adhesion and formation of a new bone [6]. PMMA-alumina composites showed improved mechanical properties [7,8]. PMMA composites have been developed for the fabrication of porous scaffolds [9], filling materials for surgery and drug delivery systems [10].

Many PMMA applications involved the use of coatings and films, which were prepared using different techniques, such as dip coating [11], sol-gel [12], casting [3], plasma polymerization [13], electrosynthesis [14], photoembossing [15], and other techniques [16]. Improved fixation of metal alloy and Ti implants has been achieved using PMMA coatings [13,17]. PMMA-$ZrTiO_4$ and PMMA-bioglass composite coatings on stainless steel allowed for enhanced corrosion resistance and improved biocompatibility [18,19]. Bioactive PMMA-bioglass composite films improved bioactivity in contact area of Ti implants and bone tissue [20]. PMMA coatings on Ti implants prevented ion release [14]. Furthermore, PMMA and PMMA composite coatings have been developed for controlled drug delivery [21,22]. New chemical modification techniques [23] allowed the fabrication of antimicrobial PMMA films. PMMA coatings and films have been developed for various functional applications in ophthalmology [24]. PMMA thin films have been designed for the fabrication of advanced eye lens [24,25] with enhanced optical, antibacterial, mechanical and wettability properties. PMMA films have also generated significant interest for biosensor technology. It has been widely reported that PMMA films offer advantages for the fabrication of biosensors for the detection of nucleic acids [26], uric acid [27], drug resistant bacteria [28] and different biomolecules [29]. Various biosensor platforms [28,29] have been developed based on PMMA films.
Increasing interest in the various applications of PMMA films and coatings has generated a need for development of new deposition techniques. Electrophoretic deposition (EPD) is a promising technique that has been used for various biomedical applications. It has been widely reported that EPD allows deposition of different anionic and cationic biopolymers, bioceramics, bioglasses, drugs, antimicrobial agents and various functional biomolecules [30–36]. The ability to co-deposit different materials by EPD offers tremendous benefits for the fabrication of composites [33,37,38]. This technique is suitable for deposition of particles of different size, ranging from several nanometers to several microns and allows the fabrication of nanocomposites and biosurfaces with desired topography [31,32]. EPD has facilitated the development of new drug delivery strategies [31]. This method is capable of depositing functionally graded and multilayer coatings [31,39,40], uniform film formation on substrates of complex shape, fabrication of patterned films and deposition on large surface area substrates. It offers benefits of high deposition rate, deposit purity and simple control of deposit thickness [33].

Despite the significant benefits of EPD, deposition of PMMA using this method faces significant challenges. EPD is based on electrophoretic motion of charged molecules or particles. However, PMMA is an electrically neutral polymer. Imparting charge to PMMA is difficult due to weak adsorption of charged dispersants on the chemically inert PMMA.

The goal of this investigation was to achieve EPD of PMMA and fabricate composite PMMA-alumina films for biomedical applications. We have developed a biomimetic approach, which was based on the use of sodium cholate (NaCh) as a solubilizing, charging and dispersing agent. NaCh is a primary bile salt, which exhibits the unique ability to solubilise different biomolecules in a human body. The experimental data presented below indicate that NaCh facilitated the solubilization of PMMA in a mixed water-ethanol solvent and formed charged complexes with PMMA macromolecules. For the first time we demonstrate the feasibility of PMMA film deposition by the EPD method. Moreover, the interaction of PMMA complexes with alumina allowed the fabrication of PMMA films on stainless steel foils. The PMMA and PMMA-alumina films showed promising performance for biomedical implant applications.

2. Experimental procedures

Sodium cholate hydrate (NaCh) and polymethylmethacrylate (PMMA, average $M_w \sim 120{,}000$) were purchased from Millipore Sigma. Al_2O_3 particles (0.13 μm) were supplied by the Baikowski Company. To fabricate the PMMA coating, 4 g L^{-1} PMMA and 1 g L^{-1} NaCh were added to a mixture of 85% ethanol and 15% deionized water. The resulting solution was continuously stirred and heated to a temperature of 55 °C. When the PMMA was fully dissolved, the solution was then slowly cooled back to room temperature.

The cell for electrophoretic deposition (EPD) contained a stainless steel anodic substrate (30 × 50 × 0.1 mm foil) and Pt counterelectrode, and the distance between the electrodes was 15 mm. A constant voltage of 30 V was used for deposition, with a deposition time of 3 min. Upon successful deposition of pure PMMA coatings, 1 g L^{-1} of Al_2O_3 particles were dispersed within the PMMA-NaCh solution. The resulting suspensions were used for the fabrication of organic-inorganic nano- composite coatings, using the same deposition conditions as the pure PMMA coatings.

Resulting coatings were thoroughly characterized using Fourier transform infrared spectroscopy (FTIR), X-ray diffraction (XRD) and scanning electron microscopy (SEM). A Bruker Vertex 70 Spectrometer was used for FTIR experiments, designed to determine if successful deposition of the pure PMMA coatings and co-deposition of Al_2O_3- PMMA had been achieved. A diffractometer equipped with a Rigaku RU200 Cu Kα rotating anode, Bruker 3-circle D8 goniometer and Bruker SMART6000 CCD area detector was used to conduct XRD experiments, to further confirm successful deposition of alumina using PMMA. Coating morphology was characterized using a JEOL JMS- 7000 F scanning electron microscope. The coating adhesion strength was measured according to the ASTM D3359-09 standard.

Osteosarcoma (Saos-2) cells (ATCC) were grown in McCoy's Modified 5A Media in 15% fetal bovine serum, and 1% penicillin-streptomycin (Life Technologies Inc.). These cells were seeded on the coated substrates at a density of 10,000 cells cm^{-2}. Well plates containing six replicates for each coating were incubated at 37.0 °C for one, three, and seven days in 5% CO_2. At each time point, the existing media solution was removed and a 1.0 mL solution of 5% alamarBlue™ (Life Technologies Inc.) in McCoy's 5A media was added for 60 min. Fluorescence was measured with a Tecan Infinite M200 Tecan at an excitation-emission wavelength of 540−580 nm to evaluate cellular metabolism.

After the seven-day cell metabolism measurements, a 300 μL solution of 0.1% triton in phosphate buffer solution (Gibco) was added to each well to lyse cells. Three replicates of 10 μL from each well were pipetted into a 96-well plate and an ALP assay was performed (Abcam). 100 μL of assay reagent solution was added to each well and the plate was incubated for 20 min at 37 °C and 5% CO_2. Absorbance readings were taken at a 405 nm wavelength using a Tecan Infinite M200 and a calibration curve was used to correlate absorbance readings to alkaline phosphatase (ALP) activity.

Datasets were screened for outliers using Dixon's Q-Test with 95% confidence. A two-way ANOVA was performed and Tukey's HSD test was used to evaluate comparisons using the statistical software package R. Statistical significance was assumed when $p < 0.05$.

3. Results and discussion

Fig. 1 shows chemical structures of PMMA and NaCh. Many functional properties of PMMA are governed by its ester groups (Fig.1A). The amphiphilic NaCh structure involves a carboxylic group and three OH groups, bonded to a steroid core, containing four rings. The convex hydrophobic side of NaCh allows its adsorption on hydrophobic particles and surfaces, whereas the concave hydrophilic side, containing OHand COO^- groups governs the NaCh solubility and anaphoretic behavior in water [41].

PMMA is a water-insoluble polymer, which is soluble in various organic solvents, such as toluene or dichloromethane. Avoiding the use of toxic organic solvents is crucial for many biomedical applications. It has been found previously that low molecular weight PMMA macro- molecules ($M_W \sim 14{,}000$) were soluble [42] in a mixed ethanol-water solvent, containing 15–25 % water. However, PMMA macromolecules with larger molecular mass are insoluble in water, ethanol and water- ethanol mixtures at room temperature. Dissolution of high molecular

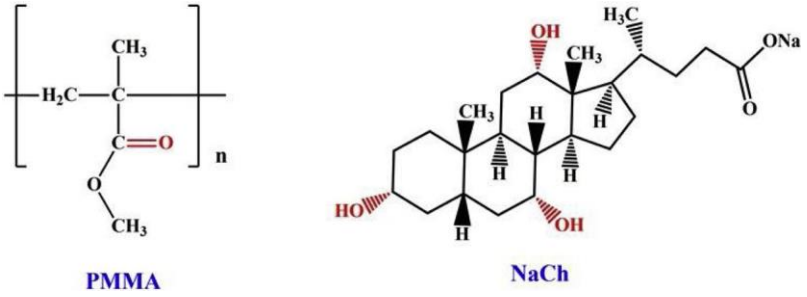

Fig. 1. Chemical structures of PMMA and NaCh.

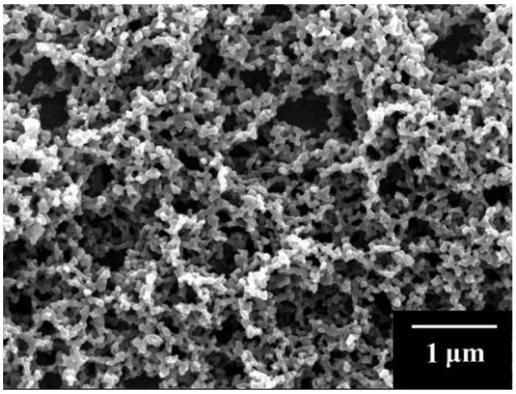

Fig. 2. SEM image of a PMMA film.

weight PMMA macromolecules in non-toxic solvents is essential to the EPD of high-quality films for biomedical applications, because polymer macromolecules with low molecular mass have been found to exhibit poor film-forming and binding properties. The typical size of polymer macromolecules used for successful fabrication of high quality films by EPD was 100,000–400,000 [37,40,43].

The molecular mass of PMMA used in this investigation was 120,000. We found that 4 g L^{-1} PMMA of such molecular mass can be dissolved in ethanol-water solvent (15 % water) at 55°C.

However, the reduction of temperature to 20°C resulted in PMMA precipitation. In contrast, the use of 1 g L^{-1} NaCh additive allowed for PMMA solubilization not only at 55°C but also after cooling to room temperature. Moreover, anodic EPD was achieved using 4 g L^{-1} PMMA solutions, containing 1 g L^{-1} NaCh. Fig.2 shows a microstructure of the film formed on a stainless-steel substrate. The film was porous and contained a network of nanoparticles. The maximum film thickness was about 2−3 µm. The adhesion strength of the film, measured according to ASTM D3359-09 standard, corresponded to 4B classification. Suc- cessful deposition of PMMA was confirmed by FTIR analysis of the film. Fig.3 compares the FTIR spectra of as-received PMMA and deposited material. The FTIR spectrum of PMMA shows an absorption at 1149 cm^{-1} related to C–O - C group symmetric stretching. The peak at 1438 cm^{-1} resulted from CH_2 bending and C−CH_3 out of plane de- formation [44]. The absorptions at 1720 cm^{-1} corresponded to C]O stretching of the $COOCH_3$ group, the band at 2951 cm^{-1} was observed due to asymmetric −CH_3 stretching [44]. Similar bands were observed in the spectrum of the deposited material.

It is important to note that PMMA is an electrically neutral polymer. Therefore, PMMA film formation by EPD provided evidence of PMMA association with cholate anions (Ch^-) in the solutions. Such association

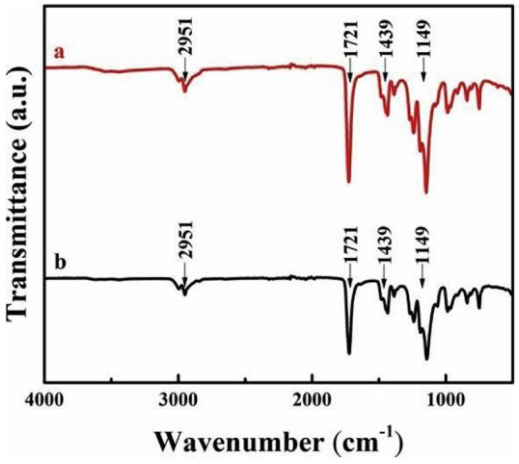

Fig. 3. FTIR spectrum of (a) as-received PMMA and (b) deposited PMMA.

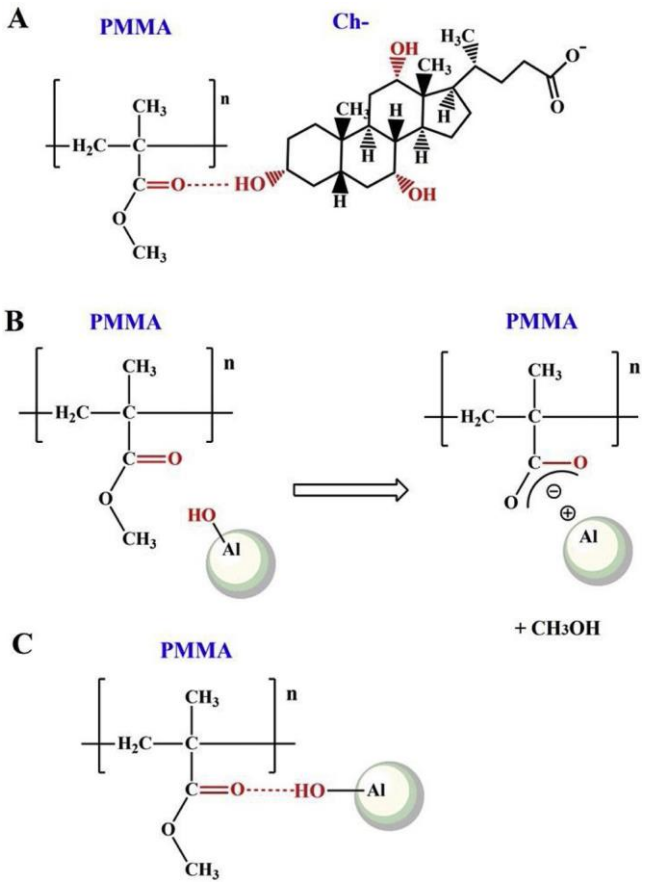

Fig. 4. (A) Hydrogen bonding of PMMA and Ch⁻, (B) interaction of PMMA with hydrated alumina surface and electrostatic interaction of PMMA and alumina, (C) hydrogen bonding of PMMA and hydrated alumina particles.

imparted a charge to PMMA, which is necessary for PMMA film EPD. The association of PMMA and Ch⁻ can result from two different mechanisms, described below or a combination of both.

It is known [45,46] that PMMA forms complexes with various organic molecules by hydrogen bonding type interactions of the PMMA carbonyl group and hydroxyl group of the organic molecules. Therefore, a hydrogen bonding mechanism can be proposed for Ch⁻ bonding to PMMA (Fig.4A). Another mechanism is related to the unique amphiphilic NaCh structure (Fig.1).

It is known [47] that bile salts, such as NaCh allow for the solubilization of cholesterol, lipids, different vitamins and other biomolecules. Moreover, NaCh allowed for excellent dispersion of carbon nanotubes and solubilization of drugs [41,48,49]. The hydrophobic side of NaCh allowed for its hydrophobic interaction with other molecules, whereas the charged hydrophilic side governed the solubility and electrokinetic properties. Adsorption of Ch⁻ imparted a negative charge to the carbon nanotubes and allowed for EPD of carbon nanotube films [49]. Therefore, the hydrophobic interactions of Ch⁻ with hydrophobic PMMA facilitated the solubilization of PMMA macro- molecules and their deposition.

Film formation involved a local pH decrease at the anode:

$$H_2O \rightarrow \tfrac{1}{2}O_2 + 2e^- + 2H^+ \quad (1)$$

followed by the protonation of adsorbed Ch⁻ and discharge:

$$Ch^- + H^+ \rightarrow HCh \quad (2)$$

Following the objective of this work, we also investigated the co- EPD of PMMA and alumina. Anodic films were obtained from alumina suspensions, containing dissolved PMMA and NaCh. Composite films

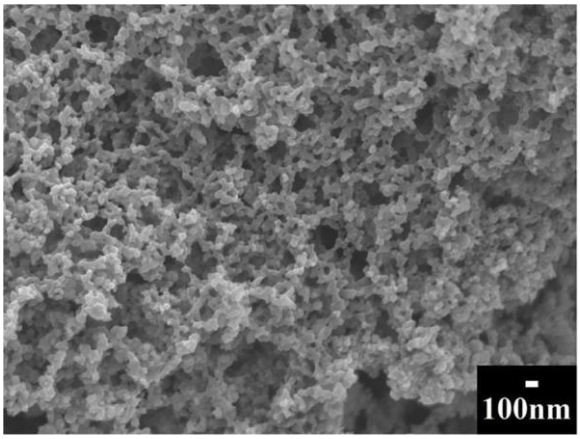

Fig. 5. SEM image of PMMA-alumina deposit on stainless steel.

with maximum thickness of about 10 μm were deposited. The films showed a porous morphology and contained submicrometre particles (Fig.5). Successful co-deposition of PMMA and alumina was confirmed by XRD and FTIR (Fig.6). The X-ray diffraction pattern of the deposited material showed well defined peaks corresponding to alumina (Fig.6A). The broad peak around 3400 cm^{-1} in the FTIR spectrum (Fig.6B) resulted from the stretching of OH groups on the alumina surface. Co- deposition of PMMA is evident from the peaks at 1723, 1436 and 1143 cm^{-1}. Similar peaks were observed in the FTIR spectra of as-received and deposited PMMA (Fig.3). Moreover, additional absorption was found at 1646 cm^{-1}. This absorption is not observed in the spectrum of PMMA (Fig.3). The absorption at 1646 cm^{-1} can result from vibrations of a carboxylic group, adsorbed on the alumina surface.

Previous investigations revealed interactions of alumina and PMMA [50–53]. It was found that surface OH groups on the alumina surface reacted with ester group of PMMA [50–53] to form a carboxylate group and methanol as a by-product (Fig.4B). This reaction resulted in ionic bond formation and strong adsorption of PMMA on alumina [50–54]. Other investigations suggested a chelating carboxylate bonding mechanism [55]. The appearance of the peak at 1646 cm^{-1} is in agreement with FTIR results of other studies, which focused on investigating the reaction between PMMA and alumina [51,53] leading to the formation of the carboxylate bonding.

This interaction between PMMA and alumina was essential for de- position of composite films. Without PMMA, alumina particles showed poor colloidal stability in NaCh solutions. As a result, EPD of alumina was unsuccessful using NaCh alone. In contrast, improved suspension stability was achieved using solutions containing both PMMA and NaCh. The 1 g L^{-1} alumina suspensions, containing 4 g L^{-1} PMMA and

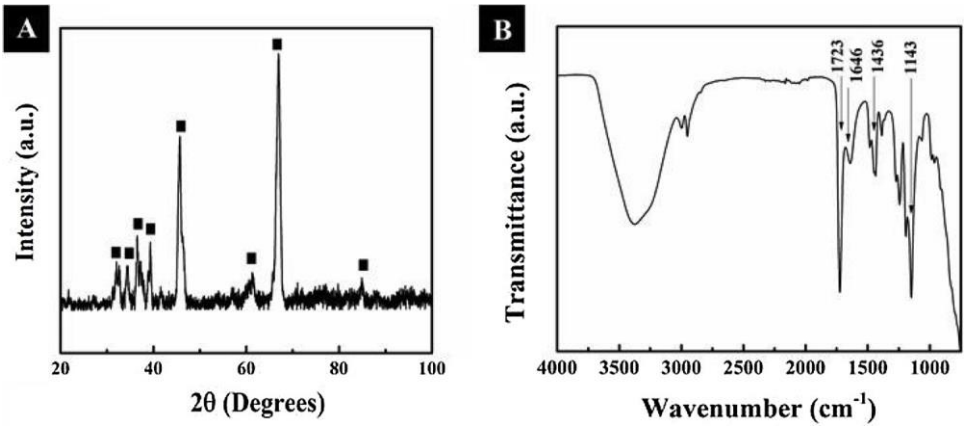

Fig. 6. (A) X-ray diffraction pattern, ■- peaks corresponding to JCPDS file 10-0425 and (B) FTIR spectrum of PMMA-alumina deposit.

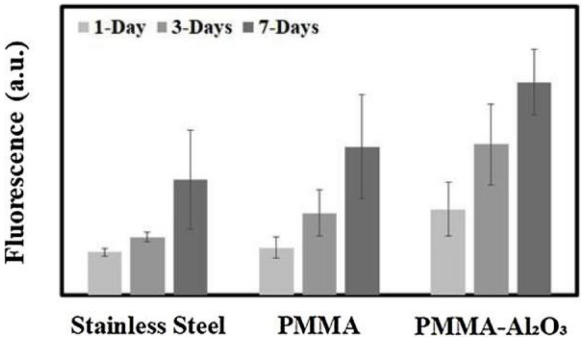

Fig. 7. Cell metabolism for Saos-2 cells seeded on coated and bare substrates, showing increased cell viability over time. PMMA-alumina films statistically outperform PMMA films and stainless steel substrates after three and seven days.

1 g L^{-1} NaCh were stable for more than 72 h. We suggest that solutions containing both PMMA and NaCh facilitated successful EPD of alumina due to PMMA-Ch- adsorption on the particle surface, which provided electrosteric dispersion and imparted a charge. PMMA-alumina inter- actions play a vital role in adsorption, which can be attributed to carboxylate-type bonding [50–54] (Fig.4B). However, PMMA can also be adsorbed on oxide particles by a hydrogen bonding mechanism (Fig.4C) [56]. The approach developed in this investigation can potentially be used for co-EPD of PMMA with other bioceramics and other functional materials. Preliminary investigations showed that PMMA can be co- deposited with hydroxyapatite, titania and zirconia.

In vitro characterization was used to assess the PMMA and composite PMMA-alumina films for potential biomedical implant applications. The metabolic results are shown in Fig.7, where cell proliferation was evident across the seven-day study period for the bare and coated stainless steel substrates. PMMA films with alumina additions showed statistically improved cell metabolism results over both the bare stainless steel substrate ($p < 0.05$) and pure PMMA ($p < 0.05$) films after three and seven days, but no significant difference was noted between the pure PMMA and the stainless steel substrate after one, three, or seven days.

ALP activity, an enzyme expressed during bone formation and indicative of a bone forming phenotype, affirmed the bioactivity of PMMA films by showing a similar trend to the metabolic assay. After seven days, the PMMA-alumina films showed greater ALP activity than both the PMMA-coated ($p < 0.05$) and uncoated stainless steel ($p < 0.05$) substrates, as shown in Fig.8. For the first time we can confirm that EPD of PMMA films on stainless steel improve the proliferation and differentiation of bone-like cells. In addition, NaCh in- corporation to enable EPD of PMMA did not appear to cause any

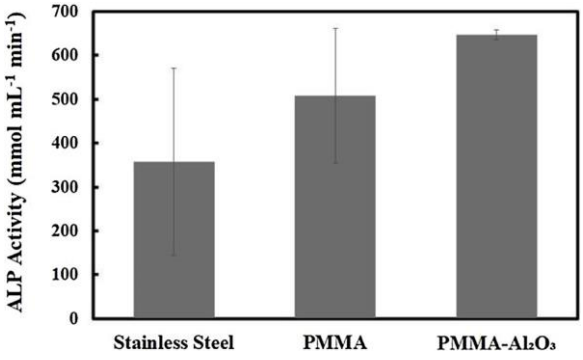

Fig. 8. ALP activity for Saos-2 cells seeded on coated and bare substrates after seven days of incubation. Each activity is statistically significant from one another.

cytotoxic effects in the PMMA composites when compared to a bare stainless steel substrates, highlighting the efficacy of NaCh as a solubilizing agent for the deposition of osteoconductive coatings.

4. Conclusion

We discovered that PMMA can be successfully dissolved in water- ethanol solvent, using NaCh as a solubilizing agent. Chemical interactions between Ch^- and PMMA allowed for charging of the PMMA molecules and subsequent film deposition using EPD. The deposition mechanism is based on anaphoresis of charged PMMA-Ch- complexes, local pH decrease at the anode, protonation and discharge of Ch^- species. Interaction between PMMA and alumina facilitated the fabrication of composite PMMA-alumina films using EPD. The feasibility studies of this work pave the way for various thin film applications of PMMA. Our new deposition strategy can potentially be used for co- deposition of PMMA with other bioceramics. The PMMA and composite films were tested for biomedical implant applications. PMMA-alumina films showed statistically improved bone-like cell metabolism results over both the bare stainless steel substrate and pure PMMA. ALP activity affirmed the bioactivity of PMMA and composite films. PMMA- alumina films showed greater ALP activity, and therefore greater osteoconductive capacity, than both the PMMA-coated and uncoated stainless steel.

Credit authorship contribution statement

A. D'Elia: Investigation, Data curation. J. Deering: Investigation, Data curation. A. Clifford: Investigation, Formal analysis, Validation. B.E.J. Lee: Investigation, Formal analysis. K. Grandfield: Methodology, Supervision. I. Zhitomirsky: Conceptualization, Supervision, Project administration, Writing - original draft.

Declaration of Competing Interest

The authors declare that they have no known competing financial interests or personal relationships that could have appeared to influ- ence the work reported in this paper.

Acknowledgement

The authors gratefully acknowledge the Natural Sciences and Engineering Research Council of Canada for the financial support. Cell culture was performed in the Biointerfaces Institute at McMaster University, and microscopy conducted in the Canadian Centre for Electron Microscopy.

References

[1] F. Ahangaran, A.H. Navarchian, F. Picchioni, Material encapsulation in poly(methyl methacrylate) shell: a review, J. Appl. Polym. Sci. 136 (41) (2019).

[2] T. Jaeblon, Polymethylmethacrylate: properties and contemporary uses in ortho- paedics, JAAOS 18 (5) (2010) 297–305.

[3] U. Ali, K.J.B.A. Karim, N.A. Buang, A review of the properties and applications of poly (methyl methacrylate)(PMMA), Polym. Rev. 55 (4) (2015) 678–705.

[4] P. Shridhar, Y. Chen, R. Khalil, A. Plakseychuk, S.K. Cho, B. Tillman, P.N. Kumta, Y. Chun, A review of PMMA bone cement and intra-cardiac embolism, Materials 9 (10) (2016).

[5] F. Rezaei, M. Abbasi-Firouzjah, B. Shokri, Investigation of antibacterial and wett- ability behaviours of plasma-modified PMMA films for application in ophthal- mology, J. Phys. D Appl. Phys. 47 (8) (2014).

[6] A.J. McManus, R.H. Doremus, R.W. Siegel, R. Bizios, Evaluation of cytocompat- ibility and bending modulus of nanoceramic/polymer composites, Journal of Biomedical Materials Research Part A: An Official Journal of The Society for Biomaterials, The Japanese Society for Biomaterials, and The Australian Society for Biomaterials and the Korean Society for Biomaterials 72 (1) (2005) 98–106.

[7] M. Mahmoudian, A.P. Marjani, R. Hasanzadeh, E. Nozad, S.M. Shishavan, H. Mohamadi, Effect of in-situ modification of α-alumina nanoparticles on me- chanical properties of poly (methyl methacrylate)-based nanocomposites for bio- medical applications, Mater. Res. Express 6 (10) (2019) 105410.

[8] N. Kyung Mok, L. Yoon Joo, K. Soo Ryong, K. Woo Teck, K. Hyungsun, K. Younghee, Bio-inspired synthesis of Al2O3/polymer composite, Mater. Sci. Forum 724 (2012) 107-10.

[9] Y. Wang, U. Gosele, M. Steinhart, Mesoporous polymer nanofibers by infiltration of block copolymers with sacrificial domains into porous alumina, Chem. Mater. 20 (2) (2008) 379–381.

[10] L.M. Rodriguez-Lorenzo, A.J. Salinas, M. Vallet-Regi, J. San Roman, Composite biomaterials based on ceramic polymers. I. Reinforced systems based on Al2O3/ PMMA/PLLA, J. Biomed. Mater. Res. 30 (4) (1996) 515–522.

[11] S. Wenyue, W. Shichao, W. Xuxu, F. Xianzhi, W. Jingning, Plasma pre-treatment and TiO2 coating of PMMA for the improvement of antibacterial properties, Surf. Coat. Technol. 205 (2) (2010) 465-9.

[12] E. Salahinejad, M.J. Hadianfard, D.D. Macdonald, M. Mozafari, D. Vashaee, L. Tayebi, A new double-layer sol–gel coating to improve the corrosion resistance of a medical-grade stainless steel in a simulated body fluid, Mater. Lett. 97 (2013) 162–165.

[13] P. Cools, N. De Geyter, E. Vanderleyden, F. Barberis, P. Dubruel, R. Morent, Adhesion improvement at the PMMA bone cement-titanium implant interface using methyl methacrylate atmospheric pressure plasma polymerization, Surf. Coat. Technol. 294 (2016) 201–209.

[14] E. De Giglio, S. Cometa, L. Sabbatini, P.G. Zambonin, G. Spoto, Electrosynthesis and analytical characterization of PMMA coatings on titanium substrates as barriers against ion release, Anal. Bioanal. Chem. 381 (3) (2005) 626–633.

[15] Q. Lin, N.F. Hughes-Brittain, C.W.M. Bastiaansen, T. Peijs, W. Wen, Responses of vascular endothelial cells to photoembossed topographies on poly(Methyl metha- crylate) films, J. Funct. Biomater. 7 (4) (2016) 33 (14 pp.).

[16] H.K. Varma, K. Sreenivasan, Y. Yokogawa, A. Hosumi, In vitro calcium phosphate growth over surface modified PMMA film, Biomaterials 24 (2) (2003) 297–303.

[17] S. Raab, A.M. Ahmed, J.W. Provan, Thin film PMMA precoating for improved im- plant bone-cement fixation, J. Biomed. Mater. Res. 16 (5) (1982) 679–704.

[18] E. Salahinejad, M.J. Hadianfard, D.D. Macdonald, S. Sharifi, M. Mozafari, K.J. Walker, A. Tahmasbi Rad, S.V. Madihally, D. Vashaee, L. Tayebi, Surface modification of stainless steel orthopedic implants by sol-gel ZrTiO4and ZrTiO4- PMMA coatings, J. Biomed. Nanotechnol. 9 (8) (2013) 1327–1335.

[19] L. Floroian, C. Samoila, M. Badea, D. Munteanu, C. Ristoscu, F. Sima, I. Negut, M.C. Chifiriuc, I.N. Mihailescu, Stainless steel surface biofunctionalization with PMMA-bioglass coatings: compositional, electrochemical corrosion studies and microbiological assay, J. Mater. Sci. Mater. Med. 26 (6) (2015) 195 (14 pp.).

[20] L. Floroian, M. Florescu, F. Sima, G. Popescu-Pelin, C. Ristoscu, I.N. Mihailescu, Synthesis of biomaterial thin films by pulsed laser technologies: electrochemical evaluation of bioactive glass-based nanocomposite coatings for biomedical appli- cations, Mater. Sci. Eng. C 32 (5) (2012) 1152-7.

[21] M.J. Kettel, E. Heine, K. Schaefer, M. Moeller, Chlorhexidine loaded cyclodextrin containing PMMA nanogels as antimicrobial coating and delivery systems, Macromol. Biosci. 17 (2) (2017).

[22] S.E. Neumann, C.F. Chamberlayne, R.N. Zare, Electrically controlled drug release using pH-sensitive polymer films, Nanoscale 10 (21) (2018) 10087-93.

[23] O. Lyutakov, I. Goncharova, S. Rimpelova, K. Kolarova, J. Svanda, V. Svorcik, Silver release and antimicrobial properties of PMMA films doped with silver ions, nano- particles and complexes, Mater. Sci. Eng. C 49 (2015) 534–540.

[24] F. Rezaei, M. Abbasi-Firouzjah, B. Shokri, Investigation of antibacterial and wett- ability behaviours of plasma-modified PMMA films for application in ophthal- mology, J. Phys. D Appl. Phys. 47 (8) (2014) 085401(10 pp.).

[25] J. Shanzuo, M. Ponting, R.S. Lepkowicz, A. Rosenberg, R. Flynn, G. Beadie, E. Baer, A bio-inspired polymeric gradient refractive index (GRIN) human eye lens, Opt. Express 20 (24) (2012) 26746-54.

[26] S.R. Nugen, P.J. Asiello, J.T. Connelly, A.J. Baeumner, PMMA biosensor for nucleic acids with integrated mixer and electrochemical detection, Biosens. Bioelectron. 24 (8) (2009) 2428-33.

[27] N. Irawati, S.W. Harun, S. Adwan, M. Alnowami, H. Ahmad, PMMA microfiber coated with Al-doped ZnO nanostructures for detecting uric acid, Microw. Opt. Technol. Lett. 57 (10) (2015) 2455-7.

[28] M. Consales, G. Quero, S. Zuppolini, L. Sansone, A. Borriello, M. Giordano, A. Venturelli, A. Cusano, Reflection-type long period grating biosensor for the de- tection of drug resistant bacteria: the opto-bacteria project, 23rd International Conference on Optical Fibre Sensors, 2 June 2014, SPIE, USA, 2014 p. 91575G (4 pp.).
[29] S.F. Wondimu, S. von der Ecken, R. Ahrens, W. Freude, A.E. Guber, C. Koos, Integration of digital microfluidics with whispering-gallery mode sensors for label- free detection of biomolecules, Lab Chip 17 (10) (2017) 1740-8.
[30] Y. Wang, I. Deen, I. Zhitomirsky, Electrophoretic deposition of polyacrylic acid and composite films containing nanotubes and oxide particles, J. Colloid Interface Sci. 362 (2) (2011) 367–374.
[31] A. Boccaccini, S. Keim, R. Ma, Y. Li, I. Zhitomirsky, Electrophoretic deposition of biomaterials, J. R. Soc. Interface 7 (suppl5) (2010) S581–S613.
[32] U. Mehana Usmaniya, V.V. Anusha Thampi, B. Subramanian, Electrophoretic de- position of bioactive glass-nanoclay nanocomposites on titanium, Appl. Clay Sci. 167 (2019) 1–8.
[33] N.M. Martinelli, M.J.G. Ribeiro, R. Ricci, M.A. Marques, A.O. Lobo, F.R. Marciano, In vitro osteogenesis stimulation via nano-hydroxyapatite/carbon nanotube thin films on biomedical stainless steel, Materials 11 (9) (2018).
[34] K. Dudek, M. Dulski, T. Goryczka, A. Gerle, Structural changes of hydroxyapatite coating electrophoretically deposited on NiTi shape memory alloy, Ceram. Int. 44 (10) (2018) 11292–11300.
[35] H. Yi, L.-Q. Wu, W.E. Bentley, R. Ghodssi, G.W. Rubloff, J.N. Culver, G.F. Payne, Biofabrication with chitosan, Biomacromolecules 6 (6) (2005) 2881–2894.
[36] L.-Q. Wu, A.P. Gadre, H. Yi, M.J. Kastantin, G.W. Rubloff, W.E. Bentley, G.F. Payne, R. Ghodssi, Voltage-dependent assembly of the polysaccharide chitosan onto an electrode surface, Langmuir 18 (22) (2002) 8620–8625.
[37] Y. Li, K. Wu, I. Zhitomirsky, Electrodeposition of composite zinc oxide–chitosan films, Colloids Surf. A Physicochem. Eng. Asp. 356 (1) (2010) 63–70.
[38] J.A. Arguello, J.M. Rojo, R. Moreno, Electrophoretic deposition of manganese oxide and graphene nanoplatelets on graphite paper for the manufacture of super- capacitor electrodes, Electrochim. Acta 294 (2019) 102–109.
[39] I. Zhitomirsky, L. Gal-Or, Formation of hollow fibers by electrophoretic deposition, Mater. Lett. 38 (1) (1999) 10–17.
[40] I. Deen, X. Pang, I. Zhitomirsky, Electrophoretic deposition of composite chit- osan–halloysite nanotube–hydroxyapatite films, Colloids Surf. A Physicochem. Eng. Asp. 410 (2012) 38–44.
[41] M.S. Ata, R. Poon, A.M. Syed, J. Milne, I. Zhitomirsky, New developments in non- covalent surface modification, dispersion and electrophoretic deposition of carbon nanotubes, Carbon 130 (2018) 584–598.
[42] R. Hoogenboom, C.R. Becer, C. Guerrero-Sanchez, S. Hoeppener, U.S. Schubert, Solubility and thermoresponsiveness of PMMA in alcohol-water solvent mixtures, Aust. J. Chem. 63 (8) (2010) 1173–1178.

[43] I. Zhitomirsky, A. Petric, Electrochemical deposition of yttrium oxide, J. Mater. Chem. 10 (5) (2000) 1215–1218.
[44] R. Huszánk, E. Szilágyi, Z. Szoboszlai, Z. Szikszai, Investigation of chemical changes in PMMA induced by 1.6 MeV He+ irradiation by ion beam analytical methods (RBS-ERDA) and infrared spectroscopy (ATR-FTIR), Nucl. Instrum. Methods Phys. Res. B 450 (2019) 364–368.
[45] W. Fu, R. Zhang, B. Li, L. Chen, Hydrogen bond interaction and dynamics in PMMA/ PVPh polymer blends as revealed by advanced solid-state NMR, Polymer 54 (1) (2013) 472–479.
[46] D. Li, J. Brisson, Hydrogen bonds in poly (methyl methacrylate)-poly (4-vinyl phenol) blends: 1. Quantitative analysis using FTi. r. spectroscopy, Polymer 39 (4) (1998) 793–800.
[47] A. Sayyed-Ahmad, L.M. Lichtenberger, A.A. Gorfe, Structure and dynamics of cholic acid and dodecylphosphocholine−Cholic acid aggregates, Langmuir 26 (16) (2010) 13407–13414.
[48] A. Clifford, I. Zhitomirsky, Aqueous electrophoretic deposition of drugs using bile acids as solubilizing, charging and film-forming agents, Mater. Lett. 227 (2018) 1–4.
[49] M. Ata, I. Zhitomirsky, Colloidal methods for the fabrication of carbon nanotu- be–manganese dioxide and carbon nanotube–polypyrrole composites using bile acids, J. Colloid Interface Sci. 454 (2015) 27–34.
[50] E. Papirer, J.-M. Perrin, G. Nanse, P. Fioux, Adsorption of poly (methylmethacry- late) on an α alumina: evidence of formation of surface carboxylate bonds, Eur. Polym. J. 30 (8) (1994) 985–991.
[51] S. Pletincx, K. Marcoen, L. Trotochaud, L.-L. Fockaert, J.M. Mol, A.R. Head, O. Karslioğlu, H. Bluhm, H. Terryn, T. Hauffman, Unravelling the chemical influ- ence of water on the PMMA/aluminum oxide hybrid interface in situ, Sci. Rep. 7 (1) (2017) 13341.
[52] G. Nunnery, E. Hershkovits, A. Tannenbaum, R. Tannenbaum, Adsorption of poly (methyl methacrylate) on concave Al2O3 surfaces in nanoporous membranes, Langmuir 25 (16) (2009) 9157–9163.
[53] K. Konstadinidis, B. Thakkar, A. Chakraborty, L. Potts, R. Tannenbaum, M. Tirrell, J.F. Evans, Segment level chemistry and chain conformation in the reactive ad- sorption of poly (methyl methacrylate) on aluminum oxide surfaces, Langmuir 8 (5) (1992) 1307–1317.
[54] Y. Grohens, M. Auger, R.E. Prud'Homme, J. Schultz, Adsorption of stereoregular poly (methyl methacrylates) on γ-alumina: spectroscopic analysis, J. Polym. Sci. Part B: Polym. Phys. 37 (21) (1999) 2985–2995.
[55] K. Hirakata, W.E. Rhine, M.J. Cima, Surface chemistry of lead titanate and its im- pact on binder removal, J. Am. Ceram. Soc. 79 (4) (1996) 1002–1008.
[56] F.-Z. Tighilt, N. Gabouze, S. Sam, S. Belhousse, K. Beldjilali, Morphology and spe- cific interaction of PMMA coating with the surface of porous silicon, Surf. Sci. 601 (18) (2007) 4217–4221.